Electrochemical Visualization of Single-Molecule Thiol Substitution with Nanopore Measurement

Published as part of ACS Measurement Science Au virtual special issue "2023 Rising Stars".

Chao-Nan Yang, Wei Liu, Hao-Tian Liu, Ji-Chang Zhang, Ru-Jia Yu, Yi-Lun Ying,* and Yi-Tao Long

Cite This: ACS Meas. Sci. Au 2024, 4, 76–80

Read Online

ACCESS | 📊 Metrics & More | 📰 Article Recommendations | 🅢ℹ Supporting Information

ABSTRACT: Reactions involving sulfhydryl groups play a critical role in maintaining the structure and function of proteins. However, traditional mechanistic studies have mainly focused on reaction rates and the efficiency in bulk solutions. Herein, we have designed a cysteine-mutated nanopore as a biological protein nanoreactor for electrochemical visualization of the thiol substitute reaction. Statistical analysis of characteristic current signals shows that the apparent reaction rate at the single-molecule level in this confined nanoreactor reached 1400 times higher than that observed in bulk solution. This substantial acceleration of thiol substitution reactions within the nanopore offers promising opportunities for advancing the design and optimization of micro/nanoreactors. Moreover, our results could shed light on the understanding of sulfhydryl reactions and the thiol-involved signal transduction mechanisms in biological systems.

KEYWORDS: Nanopore, Single-Molecule Reaction, Single-Molecule Analysis, Thiol Substitute Reaction, Reaction Kinetics
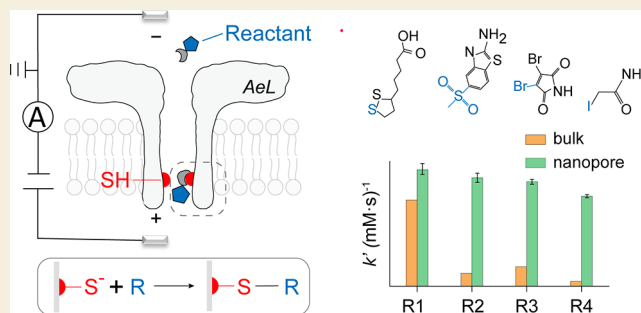
Cysteine plays an essential role in protein folding, antioxidant defense, and redox signaling.[1] The polarizable sulfur atom in the sulfhydryl group is electron-rich and highly nucleophilic,[2,3] allowing it to participate in nucleophilic substitution reactions. However, the reactivity of sulfhydryl residues is dependent on their surrounding chemical confinement within the protein structure. For example, the sulfhydryl group at 30 sites inside the DsbA protein,[4] a member of thioredoxins, exhibits identical reactivity enhancement, for which the pK_a value is around 3.0. This confinement-dependent reactivity is critical for maintaining the structure and function of proteins, including allosteric regulation and redox balance. Therefore, exploring the confined sulfhydryl reactivity is crucial for understanding sulfhydryl-participating biological processes. However, most measurements of sulfhydryl reactivity are generally conducted in vitro, which provides little information about reaction dynamics inside the confined space of proteins.[5] The conventional ensemble measurement of the sulfhydryl reactivity hardly reveals the confinement-dependent reaction dynamic of single sulfhydryl residues.[6,7] Therefore, an in situ single-molecule method for analyzing sulfhydryl-involved reactions within confined chemical environments is greatly needed.

The biological nanopore, which is assembled by pore-forming proteins, provides a platform for studying sulfhydryl reactivity at the single-molecule level.[8] A single nanopore serves not only as a confined reactor, allowing one reactant

molecule to interact with reaction sites, but also as a single-molecule sensor for measuring sulfhydryl-involved reactions.[9−19] In the typical single-molecule reaction analysis in a nanopore,[20] a single reactant molecule is driven into the nanoscale channel by electrophoresis or electroosmotic flow, generating a characteristic current when it bonds with the nanopore. The time-current recording with high spatial resolution reveals the reaction dynamics and kinetics at the single-molecule level. Similar to the structure of enzyme pockets, the nanometer-scale pore structure could shorten the diffusion distance between the captured molecule and the reaction site, providing a confined reaction environment. Therefore, measuring sulfhydryl-involved reactions inside the nanopore enables the probing the kinetics and mechanism of the thiol substitute reaction at the single-molecule level under confinement space.
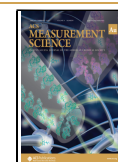
Herein, we employed a nanopore reactor K238C by introducing sulfhydryl groups inside the aerolysin (AeL) nanopore at the 238 site to visualize thiol nucleophilic
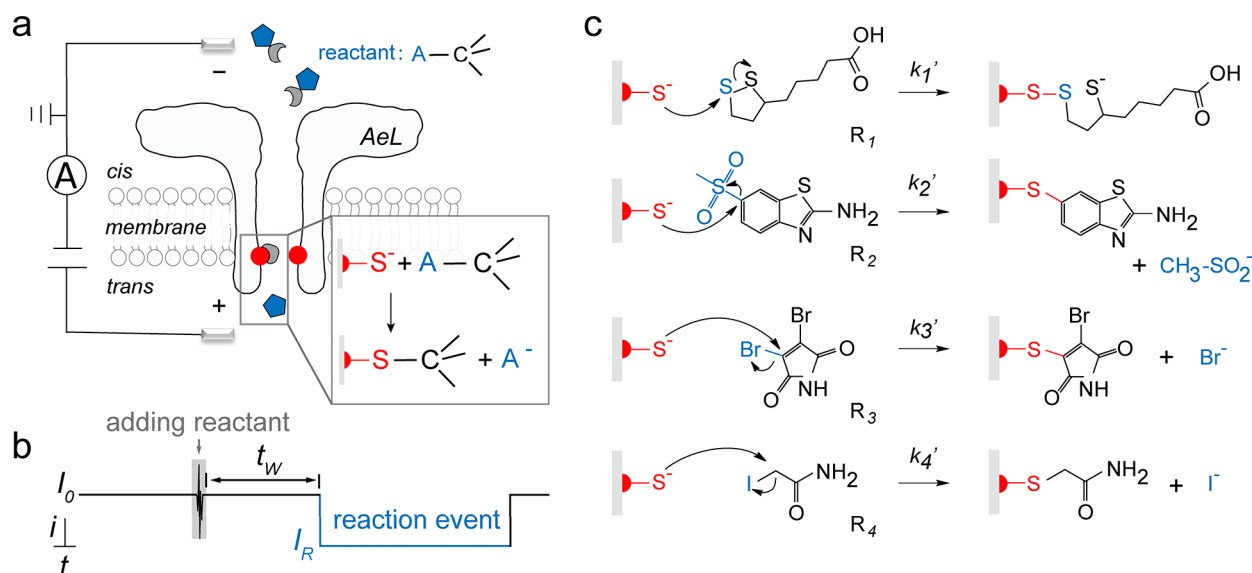
Scheme 1[a]

[a](a) Single molecule reaction in the mutant K238C AeL. Two chambers were separated by the membrane and assigned to *cis* and *trans*. The single nanopore was inserted into the membrane. The reactant was added in the *cis* chamber. (b) Representative current trace. After adding the reactant at a waiting time (t_W), the reaction event appeared with a blockade current of I_R. (c) Proposed reaction mechanism between the reactant and the K238C AeL. The reactant of (*R*)-5-(1,2-dithiolan-3-yl) pentanoic acid (reactant 1, R_1), 2-amino-6-(methylsulfonyl)benzothiazole (reactant 2, R_2), 3,4-dibromo-*N*-methylmaleimide (reactant 3, R_3), and iodoacetamide (reactant 4, R_4) gave the apparent reaction rate constant of k_1' to k_4', respectively. All experiments were performed in the buffer of 3.0 M KCl, 1.0 mM EDTA, and 10 mM Tris, at 22 ± 2 °C, pH 8.0.

substitution. By recording the characteristic current signals, we unveiled the reactivity of four distinct substrates at the single-molecule level. The results revealed a substantial enhancement of 1.3 to 1400 times in the reaction rate of thiol substitution under the confined nanopore. This study offers insights into the kinetics of thiol substitute reactions within confined protein environments, which may be beneficial to cysteine chemistry in various fields such as biocatalysis and nanotechnology.

The nanopore reactor of K238C AeL used in this work is constructed from seven identical mutant proaerolysin monomers with seven cysteines positioned at the 238 site (Scheme 1a). Herein, the sulfhydryl group, which acts as a nucleophile at position 238 providing an active site for the nucleophilic substitution (Figures S1 and S2). The open-pore current (I_0) was 90 ± 5.3 pA with root-mean-square noise (I_{RMS}) of 0.56 ± 0.15 pA when a single nanopore was inserted into the lipid bilayer at 50 mV. Previous studies reported that the reactants of R_1-R_4 with different steric hindrances and leaving groups could react rapidly with sulfhydryl groups in bulk solution under mild conditions (pH 6−8).[21−24] Considering the optimal pH condition for the substrate, herein, these reactants were respectively introduced and mixed in the *cis* chamber at pH 8.0. In order to avoid the voltage affecting the reaction kinetics inside the nanopore, a low voltage of 50 mV was applied according to our previous study.[20] Note that the *cis* chamber was grounded. The blockade current (I_R) indicates the formation of the covalent bond between the reactant molecule and K238C (Scheme 1b) (see Supplementary Experimental procedures). As a comparison to the formation of covalent bonds in the K238C nanopore, no blockage current was observed in wild type AeL (WT, without sulfhydryl group) when R_1-R_4 were added to the *cis* chamber (Figure S3). Therefore, as expected, the sulfhydryl groups of the K238C

mutant nanopore are the only reactive groups inside the nanopore for a single-molecule nucleophilic reaction.

As shown in Figure 1a, the ionic current was decreased by 9.0 ± 0.3 pA (ΔI_{R1}) when a single R_1 with a disulfide bond reacted with the sulfhydryl group of the K238C AeL. The current trace shows that the reaction signal contains irregular spikes (Figure 1a−d). According to the previous studies,[25] this current fluctuation with standard deviation (STD) of 0.38 ± 0.04 pA resulted from the dynamic changes of covalent bonds between the reactant and the nanopore (e.g., bond angle and length). Similarly, R_2 with a benzothiazole group produced ΔI_{R2} of 15.8 ± 0.5 pA as it reacted with the nanopore reactor (Figure 1b). When introducing R_3 in the nanopore reactor, the sulfhydryl group at the 238 site substituted one of the bromine atoms, leading to the connection of the maleimide molecule to the inner wall of the aerolysin nanopore through the =C−S bond (Figure 1c). The resulting ΔI_{R3} is 1.7 ± 0.3 pA. To eliminate the bias of I_0 from independent measurements, $\Delta I_R/I_0$ was introduced as the proportion of the current drop to the baseline (Figure S4). As expected, both the order of ΔI_R and $\Delta I_R/I_0$ values follow that of the cross-sectional area (CSA) of R_1-R_3, which was $R_2 > R_1 > R_3$ (Figures 1e,f and S5; Table S1). This result illustrated that the volume exclusion of the reactant inside the nanopore contributes greatly to the signal amplitude. However, R_4 with the smallest CSA (47.62 Å) among the four reactants generated the largest $\Delta I_R/I_0$ as reacted with the sulfhydryl group (Figure 1e and f). The sulfhydryl nucleophilic substitution of the iodine atom in R_4 gives the leaving group of I⁻, which may contribute to the significant current drop. To further confirm this speculation, we added the NaI solution to the K238C nanopore reactor as a control experiment. As shown in Figures 2a and S6a, I⁻ interacts with the K238C nanopore reactor strongly, resulting in the large $\Delta I_{NaI}/I_0$ of 0.19 ± 0.03. Note that this value is similar to $\Delta I_{R4}/I_0$. In contrast, the WT nanopore without the
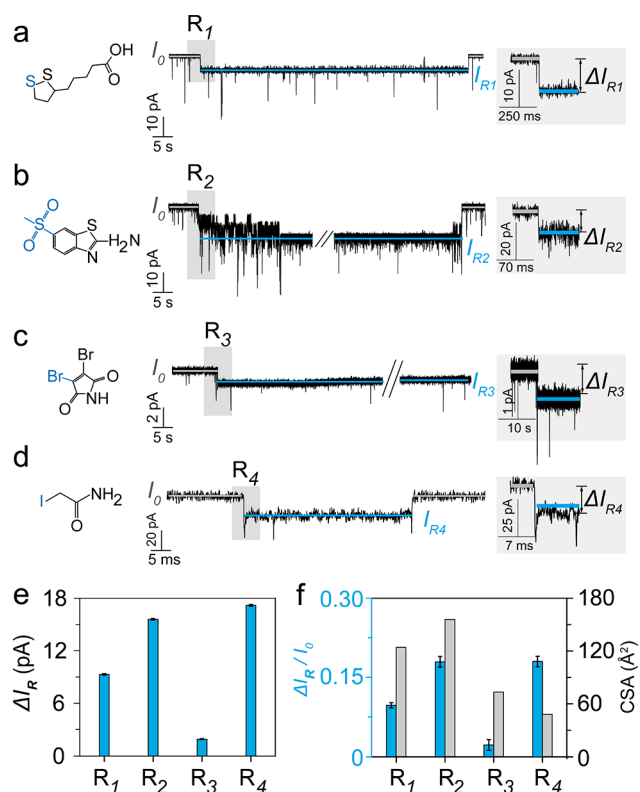
Figure 1. Representative current trace and statistical results of the reaction signals for the reactants R_1–R_4. Representative current traces of R_1 (a), R_2 (b), R_3 (c), and R_4 (d). (e) ΔI_R of the reaction signals; (f) $\Delta I_R/I_0$ (blue) of the reaction signals induced by R_1–R_4 and the corresponding CSA area (gray). Concentrations of R_1–R_4 are 2.6, 2.5, 2.5, and 50 μM in the *cis* chamber, respectively. All data were acquired under the conditions of 3.0 M KCl, 10 mM Tris, and 1.0 mM EDTA at pH 8.0. The error bars are obtained from at least three independent experiments.

Figure 2. The statistical analysis of the typical signals. (a) $\Delta I_R/I_0$ generated by reactants interacting with K238C and WT nanopore. The presence of Br$^-$ and I$^-$ is 50 mM for interacting with K238C AeL and WT AeL, respectively. The final concentration of I$^-$ is 50 mM with K238C AeL, R_3 and R_4 is 1.5 mM as interacting with K238C AeL and WT AeL, respectively. R_3 is 1.5 mM with WT AeL, R_4 is 1.5 mM with WT AeL, Br$^-$ is 50 mM and I$^-$ is 50 mM with WT AeL. (b) STD of I_0 and I_R of R_1–R_4 in K238C AeL. (c) Apparent reaction rate constants of R_1–R_4 in K238C AeL and the bulk solution. All data was acquired in the conditions of 3.0 M KCl, 10 mM Tris, and 1.0 mM EDTA at pH 8.0.

reaction site of sulfhydryl does not generate similar signals after the introduction of NaI (Figure S6b). However, Br$^-$ does not generate obvious signals as I$^-$ when NaBr was introduced to the nanopore reactor (Figure S6c). This may be caused by the interaction between the larger iodine atom and the sulfhydryl group of the K238C nanopore. Consequently, these findings further demonstrate that the R_4 molecule experiences a nucleophilic substitution reaction with the sulfhydryl group located at the 238 site. Moreover, the inclusion of the leaving group of I$^-$ within the nanopore significantly enhances the blockage amplitude of the reaction signal.

The above results revealed that the amplitude of the reaction signal would follow the volume exclusion rules, except for the strong interaction between the leaving group of I$^-$ with the nanopore reactor. The STD of the reaction signal also shows a correlation with the volume and structure of the reactant linked to the nanopore (Figure 2b). R_2, with a bulkier and rigid benzothiazole, contributed the largest STD value of 4.35 ± 0.07 pA. This is in comparison to the STD values of R_1, R_3, and R_4, all of which have flexible alkane chains or smaller volumes. Furthermore, the intensive changes in I_{R2} may potentially arise from the short-lived reactive intermediates.

Previous studies in bulk solutions[21–24] have indicated that the reaction kinetics follow the order of $R_1 > R_3 > R_2 > R_4$, from fastest to slowest (as shown in Table S1). In order to demonstrate the confined effect on the reaction kinetics inside
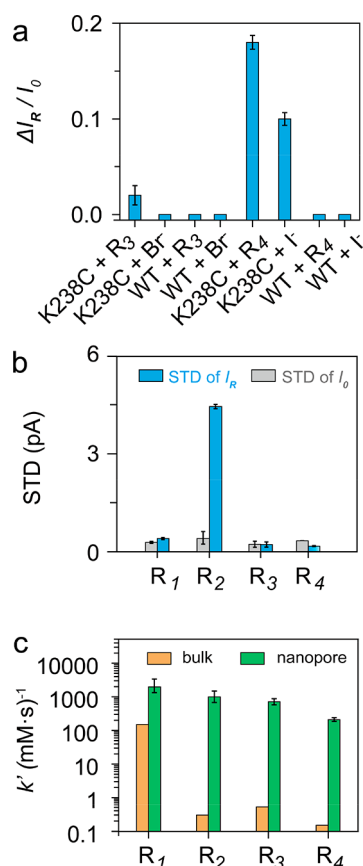
the nanopore reactor, we further calculated the kinetic constants of R_1–R_4 based on the reaction signals. We assumed the nucleophilic reaction of R_1–R_4 to one of the K238C sites follows pseudo-first-order kinetics.[26,27] The apparent reaction rate (k') between the single reactant molecule and nanopore can be determined by eq 1.

$$k' = \frac{1}{t_W[C]} \tag{1}$$

where t_W is the waiting time from the time point of the addition of the reactant to the signal occurrence (Scheme 1b) and C is the final concentration of the reactants in the *cis* chamber. It can be seen from Figure 2c and Table S1 that the k' values of R_1–R_4 inside the nanopore reactor are 1.3–1400 times higher than the reaction rate in the bulk solution. The nanoscale confinement restricts the random diffusion of the reactant, increasing the possibility of successful collisions for bond formation. This effect can accelerate the rate of the reaction, which is consistent with a previously proposed mechanism.[20,28] In contrast to the order of rate constants observed in bulk solution, it is evident that under confinement nanopore the reaction rate of R_3 is notably lower than that of

R_2. It could be explained by R_2 with the largest volume may reduce the orientational variation of the reactive group, leading to a higher probability of the effective collision to the thiol group at the K238C site in the nanopore. Therefore, the confinement effect leads to a single-molecule reaction efficiency of R_2 that is higher than R_3. These findings provide a possible explanation for the higher reaction rate observed in nanoenzymes compared to the bulk solution.

In summary, this work revealed the single-molecule kinetics of thiol substitutions with an engineered nanopore reactor. Our results showed that the characteristic current signals produced by reactants 1−4 in the nanopore are closely linked to the volume of excluded ions. Furthermore, variations in the volume and structure of the reactants led to differences in the STD. The confinement effect on the reactant within the nanopore facilitates more efficient collisions, promoting bond formation between the reactive group of the reactant and the nanopore compared to the bulk solution. Our nanopore electrochemical technique offers deeper insights into cysteine reactions within enzyme catalysis at the single-molecule level, thereby advancing our understanding of reactions taking place within confined microenvironments.

■ ASSOCIATED CONTENT

ⓢ Supporting Information

The Supporting Information is available free of charge at https://pubs.acs.org/doi/10.1021/acsmeasuresciau.3c00046.

> Experimental section, preparation and characterization of Aerolysin nanopores, CSA of reactants, interaction information between reactants 1−4 and wild-type Aerolysin nanopore (PDF)

■ AUTHOR INFORMATION

Corresponding Author

Yi-Lun Ying − *State Key Laboratory of Analytical Chemistry for Life Science, School of Chemistry and Chemical Engineering, Nanjing University, Nanjing 210023, China; Chemistry and Biomedicine Innovation Center, Nanjing University, Nanjing 210023, P.R. China;* ⓞ orcid.org/0000-0001-6217-256X; Email: yilunying@nju.edu.cn

Authors

Chao-Nan Yang − *State Key Laboratory of Analytical Chemistry for Life Science, School of Chemistry and Chemical Engineering, Nanjing University, Nanjing 210023, China*

Wei Liu − *State Key Laboratory of Analytical Chemistry for Life Science, School of Chemistry and Chemical Engineering, Nanjing University, Nanjing 210023, China*

Hao-Tian Liu − *State Key Laboratory of Analytical Chemistry for Life Science, School of Chemistry and Chemical Engineering, Nanjing University, Nanjing 210023, China*

Ji-Chang Zhang − *State Key Laboratory of Analytical Chemistry for Life Science, School of Chemistry and Chemical Engineering, Nanjing University, Nanjing 210023, China*

Ru-Jia Yu − *State Key Laboratory of Analytical Chemistry for Life Science, School of Chemistry and Chemical Engineering, Nanjing University, Nanjing 210023, China; Chemistry and Biomedicine Innovation Center, Nanjing University, Nanjing 210023, P.R. China;* ⓞ orcid.org/0000-0002-5376-3648

Yi-Tao Long − *State Key Laboratory of Analytical Chemistry for Life Science, School of Chemistry and Chemical Engineering, Nanjing University, Nanjing 210023, China;* ⓞ orcid.org/0000-0003-2571-7457

Complete contact information is available at:
https://pubs.acs.org/10.1021/acsmeasuresciau.3c00046

Author Contributions

Y.-L. Ying and Y.-T. Long conceived idea. C.-N. Yang conducted the experiment. C.-N. Yang and W. Liu analyzed the data. C.-N. Yang, W. Liu, and H.-T. Liu prepared the manuscript. R.-J. Yu, J.-C Zhang, Y.-L. Ying and Y.-T. Long wrote the manuscript.

Notes

The authors declare no competing financial interest.

■ ACKNOWLEDGMENTS

We thank Junge Li for the proaerolysin preparation and Chengbing Zhong for the instrument.

■ ABBREVIATIONS

R_1, reactant 1, (R)-5-(1,2-dithiolan-3-yl) pentanoic acid; R_2, reactant 2, 2-amino-6-(methylsulfonyl)benzothiazole; R_3, reactant 3, 4-dibromo-N-methylmaleimide; R_4, reactant 4, iodoacetamide

■ REFERENCES

(1) Sies, H.; Jones, D. P. Reactive oxygen species (ROS) as pleiotropic physiological signalling agents. *Nat. Rev. Mol. Cell Biol.* **2020**, *21* (7), 363−383.

(2) Boutureira, O.; Bernardes, G. J. L. Advances in Chemical Protein Modification. *Chem. Rev.* **2015**, *115* (5), 2174−2195.

(3) Doolan, J. A.; Williams, G. T.; Hilton, K. L. F.; Chaudhari, R.; Fossey, J. S.; Goult, B. T.; Hiscock, J. R. Advancements in Antimicrobial Nanoscale Materials and Self-Assembling Systems. *Chem. Soc. Rev.* **2022**, *51* (20), 8696−8755.

(4) Ito, K.; Inaba, K. The Disulfide Bond Formation (Dsb) System. *Curr. Opin. Struct. Biol.* **2008**, *18* (4), 450−458.

(5) Jung, S.-Y.; Liu, Y.; Collier, C. P. Fast Mixing and Reaction Initiation Control of Single-Enzyme Kinetics in Confined Volumes. *Langmuir* **2008**, *24* (9), 4439−4442.

(6) Grommet, A. B.; Feller, M.; Klajn, R. Chemical Reactivity under Nanoconfinement. *Nat. Nanotechnol.* **2020**, *15* (4), 256−271.

(7) Liu, J.; Goetjen, T. A.; Wang, Q.; Knapp, J. G.; Wasson, M. C.; Yang, Y.; Syed, Z. H.; Delferro, M.; Notestein, J. M.; Farha, O. K.; Hupp, J. T. MOF-Enabled Confinement and Related Effects for Chemical Catalyst Presentation and Utilization. *Chem. Soc. Rev.* **2022**, *51* (3), 1045−1097.

(8) Ying, Y.-L.; Hu, Z.-L.; Zhang, S.; Qing, Y.; Fragasso, A.; Maglia, G.; Meller, A.; Bayley, H.; Dekker, C.; Long, Y.-T. Nanopore-Based Technologies beyond DNA Sequencing. *Nat. Nanotechnol.* **2022**, *17* (11), 1136−1146.

(9) Luchian, T.; Shin, S.-H.; Bayley, H. Single-Molecule Covalent Chemistry with Spatially Separated Reactants. *Angew. Chem., Int. Ed.* **2003**, *42* (32), 3766−3771.

(10) Howorka, S.; Siwy, Z. Nanopore Analytics: Sensing of Single Molecules. *Chem. Soc. Rev.* **2009**, *38* (8), 2360.

(11) Liu, L.; Wu, H.-C. DNA-Based Nanopore Sensing. *Angew. Chem., Int. Ed.* **2016**, *55* (49), 15216−15222.

(12) Harrington, L.; Alexander, L. T.; Knapp, S.; Bayley, H. Single-molecule protein phosphorylation and dephosphorylation by nanopore enzymology. *ACS Nano* **2019**, *13* (1), 633−641.

(13) Qing, Y.; Ionescu, S. A.; Pulcu, G. S.; Bayley, H. Directional Control of a Processive Molecular Hopper. *Science.* **2018**, *361* (6405), 908−912.

(14) Galenkamp, N. S.; Biesemans, A.; Maglia, G. Directional Conformer Exchange in Dihydrofolate Reductase Revealed by Single-Molecule Nanopore Recordings. *Nat. Chem.* **2020**, *12* (5), 481−488.

(15) Bétermier, F.; Cressiot, B.; Di Muccio, G.; Jarroux, N.; Bacri, L.; Morozzo della Rocca, B.; Chinappi, M.; Pelta, J.; Tarascon, J.-M. Single-Sulfur Atom Discrimination of Polysulfides with a Protein Nanopore for Improved Batteries. *Commun. Mater.* **2020**, *1* (1), 59.

(16) Xue, L.; Yamazaki, H.; Ren, R.; Wanunu, M.; Ivanov, A. P.; Edel, J. B. Solid-State Nanopore Sensors. *Nat. Rev. Mater.* **2020**, *5* (12), 931−951.

(17) Tripathi, P.; Benabbas, A.; Mehrafrooz, B.; Yamazaki, H.; Aksimentiev, A.; Champion, P. M.; Wanunu, M. Electrical Unfolding of Cytochrome c during Translocation through a Nanopore Constriction. *Proc. Natl. Acad. Sci. U. S. A.* **2021**, *118*, No. e2016262118.

(18) Cairns-Gibson, D. F.; Cockroft, S. L. Functionalised Nanopores: Chemical and Biological Modifications. *Chem. Sci.* **2022**, *13* (7), 1869−1882.

(19) Wang, Y.; Zhang, S.; Jia, W.; Fan, P.; Wang, L.; Li, X.; Chen, J.; Cao, Z.; Du, X.; Liu, Y.; Wang, K.; Hu, C.; Zhang, J.; Hu, J.; Zhang, P.; Chen, H.-Y.; Huang, S. Identification of Nucleoside Monophosphates and Their Epigenetic Modifications Using an Engineered Nanopore. *Nat. Nanotechnol.* **2022**, *17*, 976−983.

(20) Liu, W.; Yang, Z.-L.; Yang, C.-N.; Ying, Y.-L.; Long, Y.-T. Profiling Single-Molecule Reaction Kinetics under Nanopore Confinement. *Chem. Sci.* **2022**, *13* (14), 4109−4114.

(21) Chen, X.; Wu, H.; Park, C.-M.; Poole, T. H.; Keceli, G.; Devarie-Baez, N. O.; Tsang, A. W.; Lowther, W. T.; Poole, L. B.; King, S. B.; Xian, M.; Furdui, C. M. Discovery of Heteroaromatic Sulfones As a New Class of Biologically Compatible Thiol-Selective Reagents. *ACS Chem. Biol.* **2017**, *12* (8), 2201−2208.

(22) Wall, A.; Wills, A. G.; Forte, N.; Bahou, C.; Bonin, L.; Nicholls, K.; Ma, M. T.; Chudasama, V.; Baker, J. R. One-Pot Thiol−Amine Bioconjugation to Maleimides: Simultaneous Stabilisation and Dual Functionalisation. *Chem. Sci.* **2020**, *11* (42), 11455−11460.

(23) Pulcu, G. S.; Galenkamp, N. S.; Qing, Y.; Gasparini, G.; Mikhailova, E.; Matile, S.; Bayley, H. Single-Molecule Kinetics of Growth and Degradation of Cell-Penetrating Poly (Disulfide)s. *J. Am. Chem. Soc.* **2019**, *141* (32), 12444−12447.

(24) Meng, J.; Fu, L.; Liu, K.; Tian, C.; Wu, Z.; Jung, Y.; Ferreira, R. B.; Carroll, K. S.; Blackwell, T. K.; Yang, J. Global Profiling of Distinct Cysteine Redox Forms Reveals Wide-Ranging Redox Regulation in C. elegans. *Nat. Commun.* **2021**, *12* (1), 1415.

(25) Wen, C.; Dematties, D.; Zhang, S.-L. A Guide to Signal Processing Algorithms for Nanopore Sensors. *ACS Sens.* **2021**, *6* (10), 3536−3555.

(26) Leonard, J. L.; Visser, T. J. Selective Modification of the Active Center of Renal Iodothyronine 5′-Deiodinase by Iodoacetate. *Biochim. Biophys. Acta. Proteins. Proteom.* **1984**, *787* (2), 122−130.

(27) Schlenoff, J. B.; Li, M.; Ly, H. Stability and Self-Exchange in Alkanethiol Monolayers. *J. Am. Chem. Soc.* **1995**, *117* (50), 12528−12536.

(28) Wordsworth, J.; Benedetti, T. M.; Somerville, S. V.; Schuhmann, W.; Tilley, R. D.; Gooding, J. J. The Influence of Nanoconfinement on Electrocatalysis. *Angew. Chem., Int. Ed.* **2022**, *61* (28), No. e202200755.